

Dielectric Properties Of Lead Potassium Lithium Niobate ($\text{Pb}_{1.85}\text{K}_{1.15}\text{Li}_{0.15}\text{Nb}_5\text{O}_{15}$) With Tetragonal Tungsten Bronze (TTB) Type Structure

E.Choukri¹, Z.Abkhar¹, Y. Gagou², M.-A. Frémy³, J.-L. Dellis², D. Mezzane¹,
M. Elmarssi², I. Luk'yanchuk² and P. Saint-Grégoire³

1 LMCN, F.S.T.G.University Cadi Ayyad Marrakech, Morocco

2LPMC, Université de Picardie, 33, rue Saint-Leu, 80039 Amiens Cédex, France

3 L2MP, UMR-CNRS 6137, Université de Toulon-Var, BP 132, 83957 La Garde Cédex, France

Abstract: A new tungsten bronze ceramic oxide, $\text{Pb}_{2-x}\text{K}_{1+x}\text{Li}_x\text{Nb}_5\text{O}_{15}$ (PKLN) ($x = 0.15$) was prepared by high temperature solid-state reaction route. Structural and electrical properties are investigated using X-ray diffraction and dielectric measurements. Room temperature XRD pattern confirms the formation of the compound with an orthorhombic crystal system. The dielectric permittivity and the loss tangent of the sample have been measured in a frequency range 1Hz–1MHz and a temperature range 35–550 °C.

Studies of dielectric properties show that the compound exhibits an anomaly at 425°C (usually called transition temperature). The electrical parameters of the material were studied using complex impedance spectroscopy showing that the compound exhibits non-Debye of relaxation process. In the paraelectric phase, activation energy was determined and the value is $E\tau = 0.68$ eV. The present ceramic is promising candidate for high dielectric constant and low loss dielectric ceramic.

Keywords: ferroelectric, tetragonal tungsten bronze, phase transition, dielectric permittivity, impedance.

Corresponding author: el.choukri@yahoo.fr

I. Introduction

Tetragonal Tungsten-bronze (TTB) compounds with general formula unit $\text{A}_2\text{BC}_2\text{Nb}_5\text{O}_{15}$ belong to an important family of dielectric materials, which display interesting ferroelectric, pyroelectric, piezoelectric, and nonlinear optic behaviors [1–4]. Fig.1 shows a schematic representation of the TTB structure projection along the [001] direction with general formula $\text{A}_2\text{BC}_2\text{M}_5\text{O}_{15}$ ($\text{M} = \text{Nb}, \text{Ta}$). The network is built up by NbO_6 octahedra sharing corners which let appear between them cavities of three types, A, B and C, characterized by coordination numbers 15, 12 and 9, respectively. The pilling up of such cavities in the [0 0 1] direction leads to the formation of square, pentagonal and triangular tunnels where the several ions fit perfectly [5]. In fact, only large ions, like K^+ , Rb^+ , Cs^+ , Pb^{2+} , Ba^{2+} or Na^+ , can be located in A or B holes, while smaller ions, for example Li^+ , must go to the C-type cavity. The great variety of TTB-type compounds is provided by the different choices of the inserted ions.

Although the prototype paraelectric phase of the whole family of $\text{A}_2\text{BC}_2\text{M}_5\text{O}_{15}$ compounds has a

tetragonal symmetry (4/mmm), the ferroelectric phase can be either of the tetragonal or of the orthorhombic symmetry. The tetragonal symmetry of ferroelectric phase when polarization P is directed along the 4th-fold symmetry axis z occurs mostly in the lead-free TTB-type compounds such as $\text{K}_3\text{Li}_2\text{Nb}_5\text{O}_{15}$ ($T_c = 430$ °C) [6]. The lead-containing compounds such as $\text{Pb}_2\text{KNb}_5\text{O}_{15}$ ($T_c = 450$ °C) [7-9] present generally an orthorhombic distortion in the ferroelectric phase provided by the strong polarizability of the Pb^{2+} ion that involves a structural anisotropy and distortion of oxygen octahedra [10]. Polarization in this case is perpendicular to the z -direction. Note, however, the special case of compound $\text{PbK}_2\text{LiNb}_5\text{O}_{15}$ ($T_c = 366$ °C) [11,12], in which the ferroelectric phase is orthorhombic whereas the polarization P is directed along z . Single crystal growth, structure and dielectric properties of $\text{Pb}_{1-x}\text{K}_x\text{Nb}_5\text{O}_{15}$ (PKN), where $x = 0.20$, has been reported by Nakano and Yamada, and Hossain [7,13].

One of the most known of these compounds is the lead potassium lithium niobate with general formula

$\text{Pb}_{2-x}\text{K}_{1+x}\text{Li}_x\text{Nb}_5\text{O}_{15}$ (PKLN). In previous studies, we have shown that $\text{PbK}_2\text{LiNb}_5\text{O}_{15}$ single crystal presents a dielectric anomaly at 366 °C and an unusual behaviour associated with intermediate phases. The ionic conduction related to lithium ions is evidenced in this material [11,12].

Impedance spectroscopy has been widely used for investigating the properties of electric materials and electrochemistry systems. No report has been found on these studies, dielectric, hysteresis, impedance and conductivity properties on ceramics of $\text{Pb}_{1,85}\text{K}_{1,15}\text{Li}_{0,15}\text{Nb}_5\text{O}_{15}$.

In this paper, we explore a new composition $\text{Pb}_{1,85}\text{K}_{1,15}\text{Li}_{0,15}\text{Nb}_5\text{O}_{15}$ of ferroelectric compounds of TTB that is called further as PKLN. This family contains an important amount of lead and therefore, similar to $\text{Pb}_2\text{KNb}_5\text{O}_{15}$ (PKN), the occurrence of ferroelectric phase is expected. In the present study, we confirm this symmetry by X-ray diffraction measurements; investigate the ferroelectric transition by dielectric measurements. The electrical parameters of the material using complex impedance spectroscopy are also examined and the activation energy is estimated in paraelectric region. The present ceramic is promising candidate for high dielectric constant and low loss dielectric ceramic.

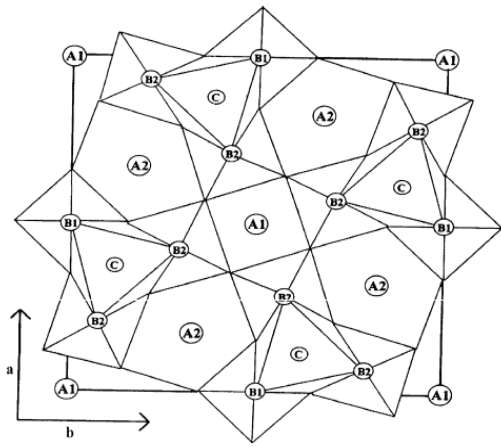


Figure 1: Schematic projection of the TTB crystalline network along the c axis

II. Sample preparation

The polycrystalline ceramic samples of $\text{Pb}_{1,85}\text{K}_{1,15}\text{Li}_{0,15}\text{Nb}_5\text{O}_{15}$ were prepared by solid-state synthesis. The starting materials were high-purity (99.9%) powders of oxides (PbO , Nb_2O_5) and carbonates (K_2CO_3 , Li_2CO_3). All these materials were weighed, mixed for 1 h. The above ingredient (carbonates and oxides) was mixed in a desired stoichiometry and grounded in methanol medium for

an hour with agate mortar. The finely crushed mixture was calcined at 900°C during 4 hours. The process has been repeated three times to achieve homogenous with single phase powder. The formation of the single phase compound was confirmed via X-ray powder diffraction (XRD) technique. The fine homogenous calcined powder then added with required organic binder poly ethylene glycol (PEG) which evaporates at low temperature to provide strength and flow ability of granules and to reduce the brittleness of sample. Powders of these compounds were initially compacted with a pressure of 2 tonnes/m² to obtain cylindrical pastille sample having in the order of 8 mm of diameter and 1mm of thickness. Finally, the obtained pellet was placed into alumina crucible and sintered during 2 h at 1150°C. The compactness value, C (defined as the ratio between the experimental density d_{exp} and theoretical density d_{theor}) obtained for sintered specimen was approximately 90%.

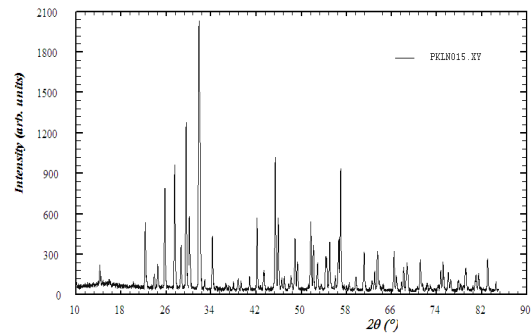


Fig. 2. X-ray diffraction patterns of $\text{Pb}_{2-x}\text{K}_{1+x}\text{Li}_x\text{Nb}_5\text{O}_{15}$ ceramic ($x=0,15$).

III. Results and discussion

III-1. X-ray Study

X-ray measurements were performed using a Bruker AXS - D8 Advanced diffractometer with a Cobalt radiations $\lambda\text{K}\alpha_1 = 1.788970 \text{ \AA}$ and $\lambda\text{K}\alpha_2 = 1.792850 \text{ \AA}$. Working in transmission (Debye-Scherrer) mode, this diffractometer is provided with a cylindrical furnace which permits us to collect X-ray diagrams versus temperatures. The sample powders were sealed in a glass capillary and the transmitted beam is focused to a punctual scintillation (NaI) detector.

The formation of the desired compound (PKLN) has been confirmed by preliminary X-ray structural analysis. The XRD pattern of PKLN compound is shown in Fig. 2. The structure was refined based on the orthorhombic structure with a space group of Cm2m. The lattice parameters has been found to be $a = 1.7919 \text{ nm}$, $b = 1.8045 \text{ nm}$ and $c = 0.3870 \text{ nm}$ at room temperature which approximately coincide with the reported values in $\text{Pb}_2\text{KNb}_5\text{O}_{15}$

($a = 1.7721$ nm, $b = 1.7983$ nm and $c = 0.3892$ nm) [14].

III-2. Dielectric measurements

Dielectric measurements were carried out by the means of a SOLARTRON SI-1260 spectrometer in the 1-106 Hz frequency domain. A source of 1Vrms was applied. The temperature variation was performed using a Linkam TS 93 hot stage allowing a temperature stability of ± 0.1 K. Samples are pastilles of ceramic. Before measurements, silver electrodes were deposited on the circular faces of the ceramic to get capacitor shaped samples.

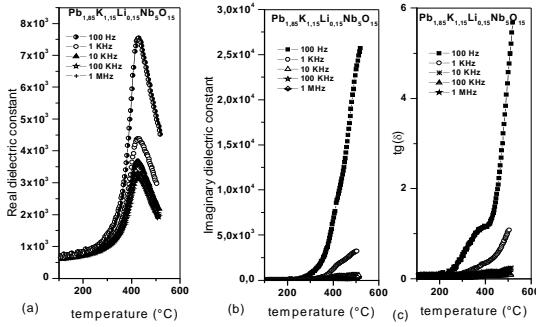


Fig. 3. (a) Temperature dependence of real dielectric constant, (b) imaginary dielectric constant and (c) dielectric loss in PKLN.

The temperature dependence of the real dielectric constant ϵ' , imaginary dielectric constant ϵ'' and $\tan\delta$ in PKLN at various frequencies are shown in Figures 3a, 3b and 3c. From Figure 3a, ϵ' , increases gradually with increase in temperature and reaches a maximum at Curie temperature, $T_c = 425$ °C. In general, the ferroelectric phase transition for TTB structure compounds possessed not only displacive characteristic but also order-disorder characteristics [15]. Also, ionic size, polarizability and electronic configuration of the ions participating in solid solution are believed to be among the factors that determine the magnitude and direction of the shift of the T_c [16]. It is observed that the room temperature dielectric constant (ϵ'_{RT}) be 560 and there was no appreciable change in its value for all frequencies studied. The value of dielectric constant at transition temperature (ϵ'_{Tc}) and at 10 kHz was about 3740. Further, the Curie temperature T_c is found to be independent of frequencies, which reveals that PKLN belong to normal ferroelectric material.

It is evident from the Fig. 3b and 3c, ϵ'' and $\tan\delta$ versus temperature, a change in slope has been observed at a particular temperature, 425 °C corresponds to the T_c value and independent of frequency. This again confirms that the material is traditional ferroelectric.

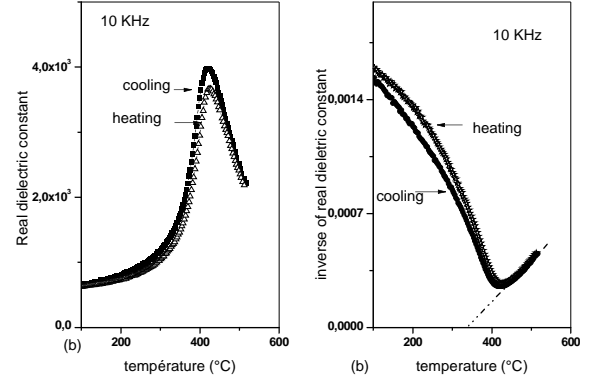


Fig. 4. Temperature dependence of the dielectric constant $\epsilon'r$ (a) and of the inverse dielectric constant $1/\epsilon'r$ (b) for PKLN at 10 KHz on cooling and on heating.

Fig. 4a shows the temperature hysteresis of the dielectric constant observed on the left ferroelectric side of the peak in $\text{Pb}_{1.85}\text{K}_{1.15}\text{Li}_{0.15}\text{Nb}_5\text{O}_{15}$ after cooling-heating cycle. The same type of hysteresis of the width 12°C was observed for all frequencies studied. We attribute this hysteresis to the first-order phase transition. Absence of discontinuity in $\epsilon'r$ and spreading of the hysteresis along all the left shoulder of the peak could signify the no uniform distribution of transition temperatures in the ceramics. We noted that a more careful study of transition in the single-crystal of $\text{Pb}_{1.85}\text{K}_{1.15}\text{Li}_{0.15}\text{Nb}_5\text{O}_{15}$ is required to confirm the nature of hysteresis and confirmed the first-order phase transition.

The thermal variation of $1/\epsilon'$ in the heating and cooling modes, shown in Fig. 4b, demonstrates the linear behavior in the paraelectric phase. Curie-Weiss law has been fitted in this region: $\epsilon'r = C/(T-T_0)$ ($T > T_C$).

where C the Curie-Weiss constant and T_0 is the Curie-Weiss temperature.

The Curie constant (C) has been found to be 4.8×10^5 K, which is a characteristic of oxygen octahedra ferroelectrics [17, 18]. The small values of T_0 ($T_C \neq T_0$) for all compositions, respect to transition temperature T_c are the characteristic property of the first-order ferroelectric phase transition. The large value of C indicates that transition is mostly of displacive type. All frequencies present the same remarks.

III-3. Impedance spectroscopy analysis

Electrical properties of electroceramics at fixed frequency don't give a whole set of properties towards the evaluation of the electric parameters as a function of temperature. Electroceramic materials give a variety of frequency dependent phenomena associated with

grain boundaries region and intrinsic properties of material [19–21].

Impedance spectroscopy studies allowed us the measurements under wide range of frequencies which will be useful to separate the contributions of electroactive regions, grain boundary and grain (bulk). Argand diagrams, imaginary part of complex impedance Z^* versus its real part allow us the determination of the bulk ohmic resistance as a function of temperature and there by temperature dependence of the conductivity [22, 23].

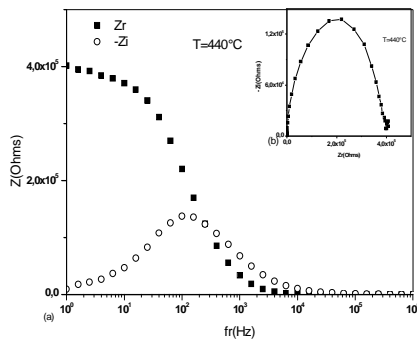


Fig. 5. (a) Frequency dependence of Zr and -Zi (b) corresponding Argand diagram (inset) for PKLN.

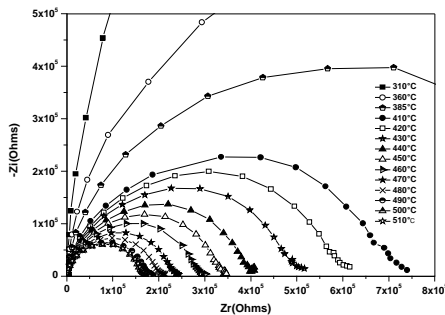


Fig. 6. Cole-Cole plots for PKLN at different temperatures.

Figures 5a and 5b show variation of Z with $\log f$ at 440 °C and corresponding Argand diagram. It is evident from the Fig. 5a that Z_r intersects Z_i at a particular frequency indicating the existence of relaxation phenomena. As the temperature increases the intersection frequency of Z_r with Z_i shifts towards high frequency side reveals the shift in relaxation frequency.

Figure 6 shows Cole–Cole plots of impedance in PKLN at several (310–510°C) temperatures in the frequency range (1–1MHz). It is evident from figure that at lower temperatures Z_i increase with increase of Z_r (linear response in Z_i). This trend indicates the insulating behavior in the material. Below 360 °C a straight-line response has been observed. As the temperature increases the slope of the line decreases

and which makes a curve towards real axis. As the temperature increases all the semicircles become smaller and shifts towards lower Z values, indicating a reduction of grain, grain boundary resistance, and negative temperature coefficient of resistance (NTCR) behavior like semi conducting materials [19–21].

All the impedance plots in PKLN exhibits the phenomena of decentralization, in which the centers of semi-circles that compose the total electric response centered below the real axis making an angle (Φ) with x-axis indicating non – Debye type relaxation process.

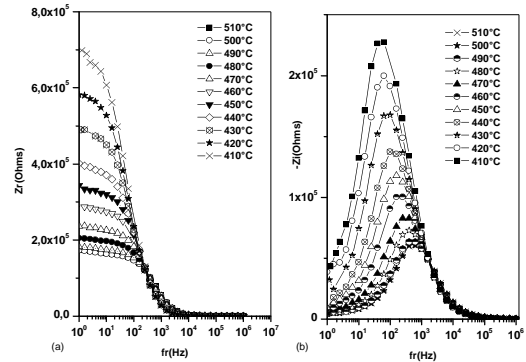


Fig. 7. Variation of (a) real (Z_r) and (b) imaginary ($-Z_i$) parts of Impedance with frequency at different temperatures in PKLN.

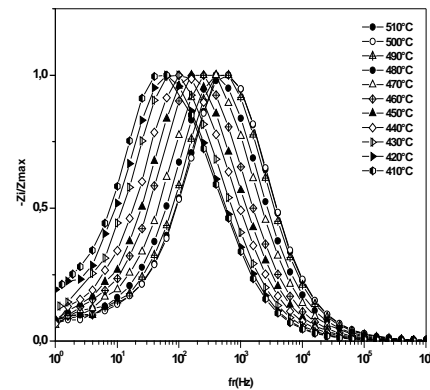


Fig. 8. Normalized imaginary parts $Z_i/Z_{i_{\max}}$ of impedance as a function of frequency for PKLN.

Figures 7a,b show the variation of real and imaginary parts of the impedance (Z_r and Z_i) as a function of frequency (1 Hz–1 MHz) at different temperatures (310 °C–510 °C) in PKLN. From the figures, the magnitude of Z_r as well as Z_i decreases with increase in frequency. This trend in Z_r indicates the increase in ac conductivity of the material, where as Z_i reveals the dependence of relaxation time in the composition. Higher impedance value of Z_r at lower

frequency side indicates the presence of space charge polarization.

As temperature increases the magnitude of Z_i decreases and the peak (Z_i max) shifts towards higher frequency side. This trend indicates increasing of relaxation time (τ), loss in the material and dependence of space charge. The value of τ has been calculated from the peak of Z_i and the asymmetric broadening of the peak suggests the spread of τ at a temperature. From the Figure 7, irrespective of the temperatures under study the Z_r as well as Z_i curves merges above 10 KHz. This is due to the reduction of space charge effect as at higher frequencies the contribution of impedance from the grain predominates over grain boundary [24].

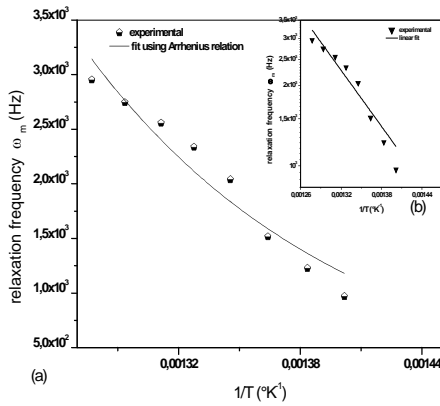


Fig. 9. Temperature dependence of relaxation frequency for PKLN.

Figure 8 shows the normalized imaginary parts Z_i / Z_i max of impedance as a function of frequency in PKLN at several temperatures. The Z_i / Z_i max parameter exhibits a peak in slightly asymmetric degree at each temperature. The plot at high temperatures indicates the triggering of another relaxation process. At the peak, the relaxation is defined by the condition, $\omega\tau_m = 1$, where, τ_m is relaxation time at the peak. The relaxation frequency plotted against inverse of temperature shown in Fig. 9, obeys the Arrhenius relation given by :

$$\omega_m = \omega_0 \exp[-E\tau/KBT] \quad (1)$$

where ω_0 and $E\tau$ are pre-exponential factor and activation energy, respectively

The relaxation frequency is a thermally activated process and the activation energy values deduced from the fit using the equation 1. From the ω_m-1/T plot, the value of $E\tau = 0.68$ eV has been found in para region ($T > 440$ °C). In previous studies, we have estimated the activation energies in $\text{PbK}_2\text{LiNb}_5\text{O}_{15}$ single crystal for paraelectric phase as 1.03eV respectively. This can be explained by fact that the ions need much more energy

for jumping in low temperature phase. The $\log\omega_m$ versus inverse of temperature response exhibited also Arrhenius behavior (Fig. 9 (b) inset). The slope calculated from the $\log\omega_m-1/T$ data, gave the same activation energies ($E\tau$) in this region.

IV. Conclusion

Ferroelectric compound of TTB structure $\text{Pb}_{1.85}\text{K}_{1.15}\text{Li}_{0.15}\text{Nb}_5\text{O}_{15}$ (PKLN) was synthesized. The phase is prepared by solid state reaction and is characterized by diffraction of X-rays and dielectric measurements. XRD analysis on ferroelectric (PKLN) ceramics confirmed homogeneous, single phase with orthorhombic structure. Phase transition temperature 425 °C in PKLN has been found from real dielectric constant versus temperature response.

All the impedance plots in PKLN exhibits the phenomena of decentralization, in which the centers of semi-circles that compose the total electric response centered below the real axis indicating non – Debye type relaxation process.

Z_i/Z_i max peak frequencies showed Arrhenius behavior and estimated activation energy 0.68 eV in para region.

This work anticipates our future investigation of ferroelectric TTB family $\text{Pb}_{2-x}\text{K}_{1+x}\text{Li}_x\text{Nb}_5\text{O}_{15}$ that will allow to study the dielectric dispersion and electric modulus method to understand the mechanism of conduction in this ceramics over wide range of frequencies and temperatures.

Acknowledgements: This work is supported by France Foreign Ministry under N°AI/MA/07/165 and by the European project FP7=IRSES=ROBOCON.

V. References

- [1] E.A. Giess, B.A. Scott, G. Burns, D.F. O’Kane, A. Segmuller, J. Am. Ceram. Soc. 52 (1969) 276.
- [2] J. Ravez, B. Elouadi, Mater. Res. Bull. 19 (1975) 1249.
- [3] J. Thoret, J. Ravaz, Rev. Chim. Minerale T24 (1987) 288.
- [4] A. Zegzouti, M. Elaatmani, Sil. Ind. 62 (7–8) (1997) 149.
- [5] M. E. Lines and A. M. Glass, Principles and applications of ferroelectrics and related materials. Ed. Clarendon Press, Oxford, p. 281, (1977).
- [6] L.G. Van Uitert, S. Singh, H.J. Levinstein, et al., Appl. Phys.Lett. 11 (1967) 161.
- [7] J. Nakano, T. Yamada, J. Appl. Phys. 46 (1975) 2361.
- [8] H. Yamauchi, Appl. Phys.Lett. 32 (1978) 599.

- [9] J. Ravez, A. Simon, P. Hagemuller, *Ann. Chim. I* (1976) 251.
- [10] Ph. Sciau, G. Calvarain, J. Ravez, *Acta Crystallogr. B* 55 (1999) 429.
- [11] Y. Gagou, D. Mezzane, N. Aliouane, T. Badèche, M. Elaatmani, M-H. Pischedda, and P. Saint-Grégoire, *Ferroelectrics* 254, 197 (2001).
- [12] Y. Gagou, M.-A. Frémy, T. Badèche, D. Mezzane, E. Choukri and P. Saint-Grégoire *Ferroelectrics*, 371, pp.1-4 (2008).
- [13] A. Hossain, In M.S. Thesis, Texas A&M University, 1984, p. 45.
- [14] K. Sambasiva Rao, P. Murali Krishna, T. Swarna Latha, D. Madhava Prasad, *Materials Science and Engineering B* 131 (2006) 127–134
- [15] M. Oualla, A. Zegzouti, M. Elaatmani, M. Daoud, D. Mezzane, Y. Gagou, P. Saint-Grégoire, *Ferroelectrics* 291 (2003) 133.
- [16] Qi YJ, Lu CJ, Zhu J, Chen XB, Song HL, Zhang HJ, et al. *Appl Phys Lett* 2005;87:082904.
- [17] T.R. Shrout, L.E. Cross, D.A. Hukin, *Ferroelectr. Lett.* 44 (1983) 325.
- [18] K. Sambasiva Rao, P. Murali Krishna, D. Madhava Prasad, Joon Hyung Lee, *Int. J. Mod. Phys. B* 21 (2007) 931.
- [19] Nobre MAL, Lanfredi S (2001) *Mater Lett* 50:322
- [20] Nobre MAL, Lanfredi S (2001) *J Phys Chem Chem Solids* 62:1999
- [21] Nobre MAL, Lanfredi S (2001) *Mater Lett* 47:362
- [22] Cole KS, Cole RH (1941) *J Chem Phys* 9:341
- [23] Bauerle JE (1969) *J Phys Chem Chem Solids* 30:2657
- [24] T.A. Nealon, *Ferroelectrics* **76**, 377 (1987)